Jurnal Ilmu Komputer dan Informasi (Journal of Computer Science and Information)
18/1 (2025), 95-101. DOI: http://dx.doi.org/10.21609/jiki.v18i1.1380

Preprocessing Impact on SAR Oil Spill Image Segmentation Using YOLOv8

Nurjannah Syakrani, Dimas Kurniawan, Wili Akbar Nugraha, Priyanto Hidayatullah, Lukmannul Hakim Firdaus, Muhammad Rizqi Sholahuddin*

Informatics Engineering, Bandung State Polytechnic, West Bandung Regency, 40559, Indonesia

E-mail: muhammad.rizqi@polban.ac.id

Abstract

Synthetic Aperature Radar (SAR) is a sensory equipment used in marine remote sensing that emits radio waves to capture a representation of the target scene. SAR images have poor quality, one of which is due to speckle noise. This research uses SAR images containing oil spills as objects that are detected using machine learning with the YOLOv8 model. The dataset was obtained from MKLab by preprocessing to improve the quality of SAR images before processing. Preprocessing involves annotating the dataset, augmenting it with flip augmentation, and filtering it using threshold and median filters in addition to a sharpen kernel that finds the optimal midway value. The default value of the YOLOv8 hyperparameter is used with addition of delta as well as subtraction of the same delta.
The implementation of preprocessing and combination of hyperparameters is examined to optimize the YOLOv8 model in detecting oil spills in SAR images. Based on 10 experimental scenarios, initial results with the original MKLab image provide an mAP50 of 49.7%. Implementing Flip augmentation alone on the data set increases the mAP50 value by 18.8%. Followed by the sharpen 1.2 kernel filter increasing the mAP50 value to 68.89%, while the median and thresholding filters tend to reduce the mAP50 value. The combination of experiments with the best results was preprocessing with flip augmentation and sharpen 1.2 kernel filter with hyperparameters: epoch 200, warmup 4.0, momentum 0.9, warmup bias lr 0.01, weight decay 0.005, and learning rate 0.000714, resulting in an mAP50 value of 68.89%. In addition, it was found that the sharpening kernel with a real number midpoint of 1.2 and combination with flipping augmentation had the greatest impact on increasing the MAP50 value in SAR oil spill image segmentation by YOLOv8.

Keywords: *SAR image with oil spill object, Flip Augmentation, Hyperparameter Configuration, Filter kernel sharpen, YOLOv8 hyperparameter default value*

1. Introduction

Oil spills are one of the environmental disasters that cause long-term negative impact on the environment. Base on [1] from 1907 to 2014, more than 7 million tons of oil have been released [2] into the environment with a total of more than 140 incidents. On April 10, 2010 there was a powerful explosion in offshore oil drilling and an estimated 4.9 million barrels of oil spilled into the sea, There were casualties of 11 officers and millions of birds died [3]. In this case, SAR imagery is very useful as information for handling ecosystem damage.

Synthetic Aperatur Radar (SAR) technology is sensory equipment installed on airplanes or satellites. SAR is generally used in marine remote sensing systems, based on microwaves, namely emitting radio waves and receiving their reflections to capture a representation of the view of a well-known target. SAR is also a powerful tool for monitoring oil spills at sea, because of its ability to be used in all weather [2].

SAR images have problems, namely unclear quality so that it is not easy to detect segmentation, one of which is caused by speckle noise [4], [5]. Noise can be reduced by applying the right type of filter. Apart from that, applying appropriate augmentation can also increase the model accuracy value [5].
Oil spill objects were segmented using the same SAR image dataset (MKLab) by comparing six deep convolutional neural network (DCNN) models: Unet, LinkNet, PSPNet, DeepLabv2, DeepLabv2(msc), and DeepLabv3+. The SAR images were resized to 320×320 pixels, and the models were trained for 600 epochs. Among the models, Unet achieved the highest performance,

with a confusion matrix accuracy value of 53.79% [6], [7] Recent studies have demonstrated the superior performance of YOLOv8 in object detection tasks using SAR imagery. Improvements to YOLOv8-GD for aircraft detection, as outlined in one study, achieved a Precision of 0.890, Recall of 0.919, and mAP50 of 0.966, leveraging advancements such as the GD mechanism, GSConv module, and WIoU loss.[8] A comparative analysis further highlights YOLOv8 as the fastest and most accurate design among four architectures, with a mAP50 of 0.62 on SAR test data, outperforming YOLOv5 (0.58 mAP50), EfficientDet (0.47 mAP50), and Faster R-CNN (0.41 mAP50).[9] Together, these findings establish YOLOv8's suitability for remote sensing applications, offering significant benefits in speed, accuracy, and scalability for complex SAR datasets.This research aims to obtain better accuracy in terms of detecting oil spills at sea by first improving SAR images using filters, augmentation and a different model, namely YOLOv8. In addition to being relatively new, the YOLOv8 model's popularity stems from its ability to blend accuracy with speed [10] and supports image processing tasks such as object detection, segmentation, pose estimation, tracing, and classification [11].

2. Methods

This research method consists of four main stages, each of which has several activities, as shown in Figure 1 The testing results are then analyzed and concluded.

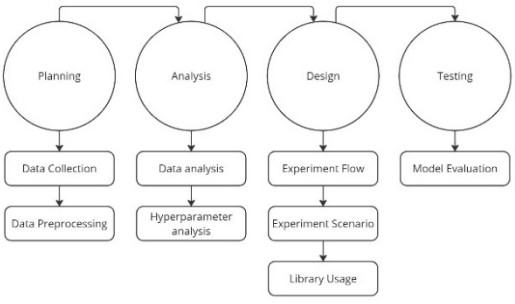

Figure 1. Experimental stages.

3. Planning

Planning as the first stage of the research method is related to data, namely collection SAR images and image preprocessing.

3.1 Data Collection

The SAR image dataset obtained from MKLab is publicly available by open request (https://mklab.iti.gr/results/oil-spill-detection-dataset/). This dataset consists of 1,112 images measuring 1,250 x 650 pixels, having a total of 2,634 oil spill objects. Each image consists of 1 to 5 different objects as listed in Table 1.

Table 1. Object and colors images

No	Object Name	Color
1	Oil	Cyan
2	Look-Alikes	Red
3	Ship	Orange
4	Sea	Black
5	Land	Green

In Figure below is a SAR image consisting of 5 objects. SAR images that are similar to an oil spill are marked with a red line, while the oil spill object is colored cyan, and so on. Look-Alikes are specifically objects generated by, among other things, winds blowing at low speeds (<2m, generally 3m – 14m) above the sea surface and phytoplankton, or a group of fish below the sea surface that are caught as objects by radar.

The slow-moving wind over sea waves acts like a mirror that reflects the radar signal in reverse direction and is received back by the radar as a Look-Alikes object in the image [12].

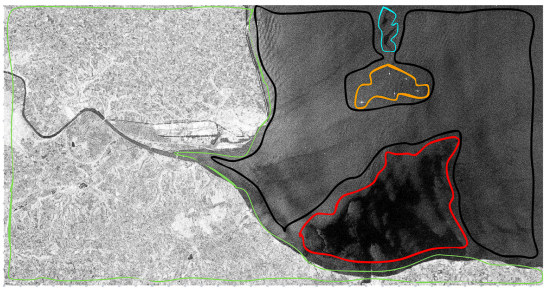

Figure 2. SAR image contains five objects.

3.2 Data Preprocessing

Pre-processing on the SAR image dataset was carried out using the polygon tools on the Roboflow website by adding annotations to oil spill objects contained in the SAR images. The annotation process for 1,112 SAR images produced only 1,110 images. This is because Roboflow automatically reads and deletes one of the same images. Figure 3 and Figure 4 show the original image and the labeling results.

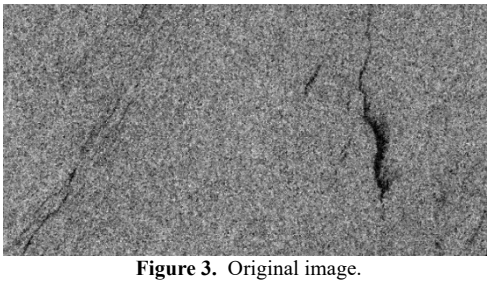

Figure 3. Original image.

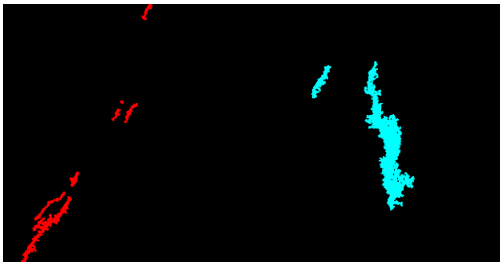

Figure 4. SAR image with two annotated objects.

The annotated image is then filtered to reduce noise. and then there are three filter methods used, namely sharpen kernel, median and thresholding, (1) A filter that uses a sharpen kernel, is a type of spatial filter that functions to regulate the light contrast at each pixel by applying a 3x3 kernel [11], (2) The median filter is one type of non-linear filter. Since the median filter does not rely on values that are substantially different from the norm for the neighborhood, it is particularly good in preserving the image features. Each window's pixels are arranged in ascending order, and the value of the pixel in the middle is chosen to be the new value for that specific pixel. To assess how well the mean and median filters reduced the speckle noise common in radar images, such as SAR images, a 3X3 pixel image window size was used. The simulation's findings demonstrate that median filters outperform other filters for both the MSE and PSNR when there is a lot of speckle noise in the SAR image [13], and (3) Thresholding, this filter replaces each pixel in the image so that if the value of a particular pixel is greater than the threshold, that pixel is classified as background and set to white, whereas if the pixel value is classified below the threshold, it is classified as foreground and set to black [14]. The effects of the 3 catagories of filters are part of the analysis.

0	0	0
0	1.2	0
0	0	0

0	0	0
0	1.3	0
0	0	0

Figure 5. Two new sharpening kernels with real numbers.

After the filter process, data augmentation is applied to increase image variance. More data increases machine learning performance. One of the geometric augmentation techniques is flipping or mirroring both horizontally and vertically [7]. Horizontal flipping is more popular and realistic to use because it changes the direction of the image object from left to right or vice versa while vertical flipping flips the image object from top to bottom [12]. Flipping augmentation is very appropriate for application since SAR images contain objects that remain unaffected by horizontal or vertical flipping. There are 1110 SAR images consisting of 681 for training, 111 for validation and 115 for testing to become 2269 due to flipping, according to formula (1) below [2]. Spesifically, the training image is tripled due to the original image, plus the results of horizontal flipping and vertical flipping.

$$T_{\text{aug}} = (N_{\text{train}} \times 3) + N_{\text{val}} + N_{\text{test}} \quad (1)$$

4. Analysis

The analysis stage aims to define the needs and process flow of the model. This analysis includes experimental data requirements and hyperparameter analysis

4.1 Analysis Data Requirements

The dataset that will be used in the experiment is chosen through data requirements analysis. The number of SAR images is 1110 and those containing oil spill objects are 873.

Figure 6 illustrates the structure of the input dataset required for this research, comprising SAR images in the .jpg format and their corresponding annotation files in the .txt format. Each SAR image must have a matching annotation file with the same name (e.g., image1.jpg and image1.txt) to ensure accurate pairing during processing. These files are organized into separate folders, one for images and another for annotations, to comply with YOLOv8's dataset requirements. This structured approach is essential for seamless integration and processing, enabling the YOLOv8 model to accurately map each image to its respective annotations for training and evaluation.

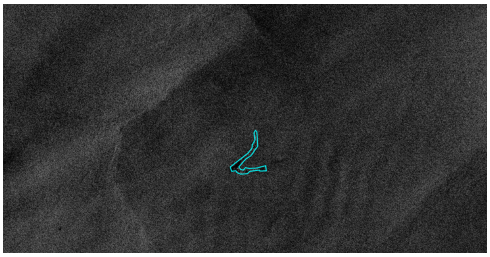

Figure. 6 Image SAR and annotations.

Figure 7 provides detailed annotation information representing the characteristics of an oil spill object

in a dataset. The annotation includes the class ID (Cls ID), where the value "0" signifies the object belongs to the oil spill category. Additionally, the bounding box is described by four numerical values indicating its position and size within the image, with its dimensions defined relative to the normalized image size. This structured annotation format facilitates accurate object detection and classification in image processing tasks.

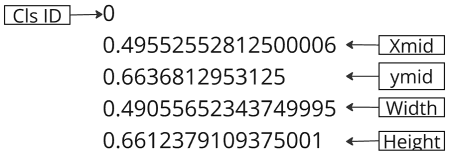

Figure 7. Annotations File Description.

4.2 Hyperparameter Analysis

Hyperparameter analysis aims to determine a combination of hyperparameters so that the model has better accuracy. The default hyperparameters of the YOLOv8 version add a certain delta (Up) and subtract the same delta (Down) as shown in Table 2. Using batch 16 and epoch 200, the combination of hyperparameters is tested in stages to determine which one is the best to support the model.

Table 2. Hyperparameters configuration.

Hyperparamaters	Default	Down	Up
weight_decay	0.0005	0.00005	0.005
warmup_epochs	3.0	2.0	4.0
warmup_momentum	0.8	0.7	0.9
warmup_bias_lr	0.1	1.0	0.01
momentum	0.937	0.927	0.947
optimizer	AdamW	AdamW	AdamW
lr (learning rate)	0.01	0.1	0.001
Hyperparamaters	**Default - auto**	**Down- auto**	**Up- auto**
weight_decay	0.0005	0.00005	0.005
warmup_epochs	3.0	2.0	4.0
warmup_momentum	0.8	0.7	0.9
warmup_bias_lr	0.1	1.0	0.01
momentum	0.9	0.9	0.9
optimizer	AdamW	AdamW	AdamW
lr (learning rate)	0.000714	0.000714	0.000714

5. Design

Design is needed to experiment using original SAR images as well as preprocessed images and hyperparameter configurations. The design stage consists of three subprocesses.

5.1 Experiment Flow

This research carried out an experiment in developing a model following the path that has been created as in Figure 8.

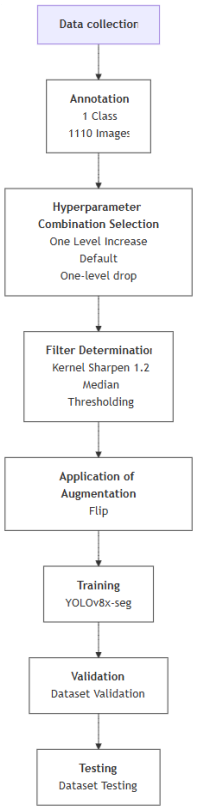

Figure 8. Model development flow.

5.2 Experimental Scenario

This research experiment uses the YOLOv8 model for model training with epoch 200, batch 16. The first experiment uses (1) the default hyperparameters, (2) all parameters in the up column and (3) all parameters in the down column in Table 3 above, for the original SAR image. The best hyperparameter values are used to process SAR images that have been preprocessed. There are 4 types of filters, namely Kernel Sharpen 1.2, Kernel Sharpen 1.3, Median, and Thresholding as well as flip augmentation to support the improvement of SAR images as input. as in Figure 9,10,11 show SAR original image and effect of sharpening. In this case there are 10 experimental scenarios.

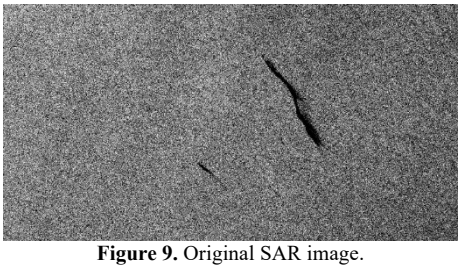

Figure 9. Original SAR image.

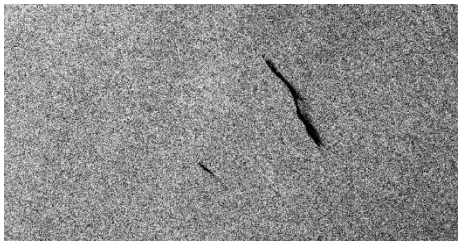

Figure 10. SAR image and kernel sharpening 1.2.

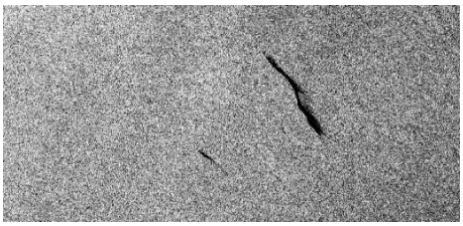

Figure 11. SAR image and kernel sharpening 1.3.

In the preprocessing stage, filters are applied using OpenCV and NumPy, which provide robust tools for image processing and numerical operations. For model development, the Ultralytics library is utilized, specifically leveraging YOLOv8. As the latest iteration in the YOLO series, YOLOv8 introduces advanced features such as an anchor-free detection head and state-of-the-art backbone and neck architectures, enhancing both detection accuracy and processing speed. This integration ensures efficient development, enabling precise object detection and classification.

5.3 Model Evaluation

Evaluation of the model to obtain oil spill detection accuracy in the form of the mAP or mAP50 metric, namely mean average precision calculated at an intersection over union (IoU) threshold of 0.50. mAP with a high value indicates that the model can identify objects with a good level of accuracy. The mAP equation is

(2) where APi is the average precision in class i and N number of class. [15]

$$\text{mAP} = \frac{1}{\text{N}} \sum_{\text{i}=1}^{\text{N}} \text{AP}_\text{i} \qquad (2)$$

5.4 Testing

Testing the original SAR image as a dataset uses a composition of 80% of the image for training, 10% for validation and 10% for testing. Testing using Flip augmentation preprocessing, the composition of the dataset changes to 80% images for training, 10% for validation and 10% for testing. The images used in training, validation and testing are different. The following is the number of SAR images used as input for the experiment as in figure 12 and 13.

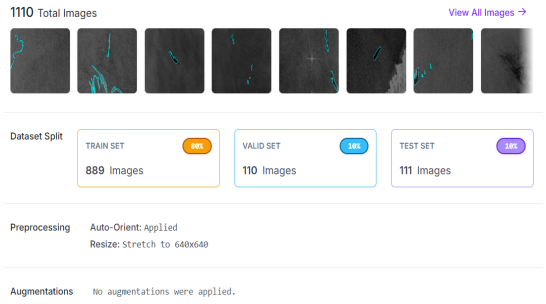

Figure 12. Split dataset original.

Figure 13. Split dataset preprocessing.

To test a model, one can provide it with instructions to forecast previously unutilized synthetic aperture radar (SAR) images. Figure 14 is an example of SAR image prediction output by the YOLOv8 model.

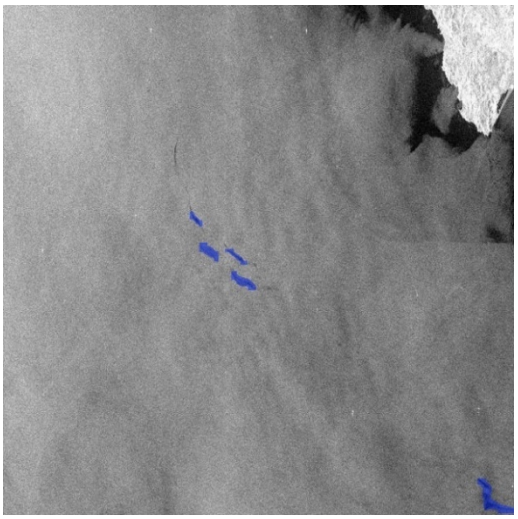

Figure 11. Example of model prediction result on SAR imagery.

Figure 14 illustrates the YOLOv8 model's capacity to generate precise segmentation masks for objects within SAR imagery. The model demonstrates robust performance in localizing oil spills with high precision, creating detailed masks that demarcate their spatial boundaries. This demonstration highlights the model's potential for real-world applications, such as maritime surveillance, environmental monitoring, and disaster management.

6. Result and Discussion

Experiment results with the YOLOv8 model, default epoch is 200, batch 16 starting with the original SAR image provide Table 3.

Table 3. Hyperparameter effect in original SAR image.

Hyperparameter	P	R	mAP50
Default	0.161	0.00952	0.0555
Up	0.683	0.397	0.477
Down	0	0	0
Default-auto	0.564	0.473	0.49
Down-auto	0.692	0.406	0.481
Up-auto	0.599	0.474	0.497

The best results are given all the *up-auto* values of the hyperparameters as in Table ,then the auto hyperparameters are used for the filtered SAR image as listed in Table 4. Implementation of flip augmentation of mAP50 on the original image provides an increase in value of (0.685-0.497) = 0.188 or 18.8%. It can be seen in Table . This demonstrates that accuracy increases with the number of training datasets. Furthermore, the down parameter value led to a complete degradation of the Precision-Recall (PR) metric (resulting in PR = 0), attributable to an excessively high learning rate (0.1) and momentum coefficient (0.927).

Table 4. Flip augmentation effect.

Image	Augmentation	P	R	mAP50
Default-auto	Flip	0.75	0.615	0.672
Dow-auto	Flip	0.748	0.636	0.676
Up-auto	Flip	0.719	0.651	0.685

Implementation of preprocessing with four types of filters gives the results in Table 5. The highest mAP50 value was obtained on SAR images filtered with Kernel sharpen 1.2.

Table 5. Filter effect.

Filter	P	R	mAP50
Kernel sharpen 1.2	0.636	0.448	0.493
Kernel sharpen 1.3	0.6	0.476	0.478
Median	0.67	0.403	0.459
Otsu Thresholding	0.604	0.314	0.326

When applied to SAR images corrupted by speckle noise, spatial filtering often fails to increase the mAP50 value compared to the original image. One hypothesis is that spatial filters (e.g., mean or median filters) primarily smooth noise at the cost of blurring fine details, which may degrade features critical for object detection tasks.

Furthermore, adding flip augmentation to the filtered SAR image gives the highest mAP50 produced by the image that applies the sharpen 1.2 kernel filter and flip augmentation. It can be seen in Table 6.

Table 6. Flip augmentation and filter application result.

Filter	Augmentation	P	R	mAP50
Kernel sharpen 1.2	Flip	0.754	0.651	0.689

Figure 15 shows the difference in YOLOv8 results for original SAR images and SAR images that have been preprocessed.

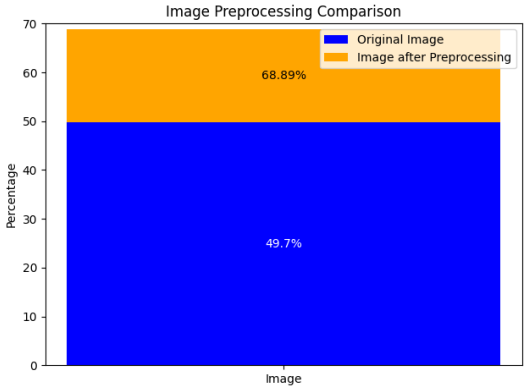

Figure 12. Comparison of mAP50 value of original image and after preprocessed image.

7. Conclusion and Suggestion

According to this study, the model that produced the greatest results in SAR image preprocessing using a sharpen kernel filter and flip augmentation had the highest mAP50 of 68.89% (= 0.689). Flip augmentation generally enhances the mAP50 metric. For instance, augmenting the original SAR image resulted in an 18.8% increase in mAP50, while applying a sharpened 1.2 kernel filter to the SAR image led to a 19.2% improvement. In contrast, the use of median and threshold filters typically decreases the mAP50 value.

This study also introduces a new sharpening kernel with a real number midpoint, especially a midpoint of 1.2 which combined with flipping augmentation has an impact on the highest MAP50 improvement in SAR oil spill image segmentation via YOLOv8.

While the proposed model demonstrates robust performance in detecting oil spills within the tested SAR dataset, its generalizability to broader operational scenarios remains unverified. The study's evaluation was confined to a single dataset due to the scarcity of publicly accessible, annotated SAR datasets. This limitation underscores the need for validation across multi-domain SAR datasets to confirm the model's adaptability to varying imaging conditions, sensor configurations, and geographical contexts.

To address this constraint, future research can employ synthetic data augmentation techniques such as leveraging generative adversarial networks (GANs) trained on limited real-world samples—to mitigate dataset scarcity while preserving the statistical fidelity of SAR speckle patterns. Further exploration should also systematically evaluate preprocessing pipelines for SAR imagery,

including (1) advanced augmentation strategies beyond geometric transformations (e.g., radiometric perturbations simulating varying incidence angles or polarization effects), and (2) frequency-domain filtering approaches (e.g., wavelet-based denoising or Fourier-domain adaptive thresholding) to suppress speckle noise without sacrificing structural granularit.

References

[1] P. Li, Q. Cai, W. Lin, B. Chen, and B. Zhang, "Offshore oil spill response practices and emerging challenges," *Mar Pollut Bull*, vol. 110, no. 1, pp. 6–27, 2016, doi: 10.1016/j.marpolbul.2016.06.020.

[2] X. Ding, X. Li, P. Liu, Y. Wei, S. Huang, and J. Zhong, "Oil Spill Detection In Sar Images Using Multiscale Normalized Cut Segmentation," 2014, pp. 1829–1831.

[3] J. Timperley, "The biggest oil spill in US history: What we've learned since Deepwater Horizon." [Online]. Available: https://www.bbc.com/future/article/20240905-have-we-improved-oil-spill-clean-ups-since-bp-deepwater-horizon

[4] P. Kaushik and S. Jabin, "A comparative study of pre-processing techniques of SAR images," presented at the 2018 4th International Conference on Computing Communication and Automation, ICCCA 2018, 2018, pp. 1–4. doi: 10.1109/CCAA.2018.8777710.

[5] R. S. Passa, S. Nurmaini, and D. P. Rini, "YOLOv8 Based on Data Augmentation for MRI Brain Tumor Detection," *Scientific Journal of Informatics*, vol. 10, no. 3, p. 363, 2023, doi: 10.15294/sji.v10i3.45361.

[6] M. Krestenitis, G. Orfanidis, K. Ioannidis, K. Avgerinakis, S. Vrochidis, and I. Kompatsiaris, "Oil spill identification from satellite images using deep neural networks," *Remote Sens (Basel)*, vol. 11, no. 15, pp. 1–22, 2019, doi: 10.3390/rs11151762.

[7] R. Hasimoto-Beltran, M. Canul-Ku, G. M. Díaz Méndez, F. J. Ocampo-Torres, and B. Esquivel-Trava, "Ocean oil spill detection from SAR images based on multi-channel deep learning semantic segmentation," *Marine Pollution Bulletin*, vol. 188, p. 114651, Mar. 2023, doi: 10.1016/j.marpolbul.2023.114651.

[8] Y. Cai, Y. Zhao, S. Wen, and J. Feng, "Improved YOLOv8 SAR Image Aircraft Object Detection Method," in *2024 7th International Symposium on Autonomous Systems (ISAS)*, Chongqing, China: IEEE, May 2024, pp. 1–6. doi: 10.1109/ISAS61044.2024.10552553.

[9] R. Glue, "YOLOv8, EfficientDet, Faster R-CNN or YOLOv5 for remote sensing." [Online]. Available: https://medium.com/@rustemgal/yolov8-efficientdet-faster-r-cnn-or-yolov5-for-remote-sensing-12487c40ef68

[10] J. Terven and D. Cordova-Esparza, "A Comprehensive Review of YOLO: From YOLOv1 and Beyond." [Online]. Available: http://arxiv.org/abs/2304.00501

[11] S. Krig, "Image Pre-Processing," in *Computer Vision Metrics*, Cham: Springer International Publishing, 2016, pp. 35–74. doi: 10.1007/978-3-319-33762-3_2.

[12] Y. Zhang, Y. Li, and H. Lin, "Oil-Spill Pollution Remote Sensing by Synthetic Aperture Radar," in *Advanced Geoscience Remote Sensing*, InTech, 2014. doi: 10.5772/57477.

[13] K. Griffith S., G. Akpeko, and A. K. E. Isaac, "On the Performance of Filters for Reduction of Speckle Noise in SAR Images Off the Coast of the Gulf of Guinea," *International Journal of Information Technology, Modeling and Computing (IJITMC)*, vol. 1, no. 4, pp. 41–50, 2013, doi: 10.5121/ijitmc.2013.1405.

[14] A. Kieri, "Context Dependent Thresholding and Filter Selection for Optical Character Recognition," 2012.

[15] S. Minaee, Y. Boykov, F. Porikli, A. Plaza, N. Kehtarnavaz, and D. Terzopoulos, "Image Segmentation Using Deep Learning: A Survey," *IEEE Trans Pattern Anal Mach Intell*, vol. 44, no. 7, pp. 3523–3542, 2022, doi: 10.1109/TPAMI.2021.3059968.